Available online at www.sciencedirect.com
ScienceDirect
International Journal of Mass Spectrometry 271 (2008) 51–57
International Journal of Mass Spectrometry
www.elsevier.com/locate/ijms

Electron impact ionization of metastable rare gases: He, Ne and Ar

M. Asgar Ali, P.M. Stone *

National Institute of Standards and Technology, Gaithersburg, MD 20899, United States

Received 29 August 2007; received in revised form 12 October 2007; accepted 12 October 2007
Available online 23 October 2007

Abstract

Cross sections for ionization of atoms by electron impact are important quantities for modeling of low temperature plasmas and gas discharges. Although experimental and theoretical studies of ionization of atoms from their ground levels have been extensive, much less information is available about the larger cross sections for ionization from excited levels. We use the Binary–Encounter–Bethe (BEB) method of Kim and Rudd to calculate ionization cross sections from the 1s2s ^{3}S level of He, the $2p^5 3s$ ^{3}P levels of Ne, and the $3p^5 4s$ ^{3}P levels of Ar. We compare our results with the few available experimental results and with results from other theoretical methods.
Published by Elsevier B.V.

Keywords: Ionization; Electron; Metastable; Rare gas

1. Introduction

Cross sections for electron impact ionization of atoms and molecules are basic data needed for modeling of gas discharges and plasmas, and for planetary atmospheric physics. Ionization of atoms and ions from their ground levels has been extensively studied experimentally and theoretically [1–11]. The ionization cross sections of ground level rare gas atoms have been measured repeatedly [12,13] in view of their importance in plasma diagnostics [14–16] and as tests for the performance of advanced collision theory and of simplified collision theory based on bound level wave functions.

Only a few experimental studies have been made of ionization of rare gas atoms from excited levels. As the ionization cross sections from atoms in excited levels are larger than that of ground level atoms, excitation coupled with subsequent ionization enhances the total ionization rate. In many laboratory and astrophysical plasmas, metastable populations are considerable and ionization from metastable populations is a major contributor to the ionization rate and the electron energy distribution. Cross sections for ionization from He [17,18], Ne [19,20] and Ar [20] metastable levels have been measured over a limited energy range. Several theoretical studies of these cross sections have been made using advanced methods or simplified models [21–30].

In the present paper, we report electron impact ionization cross sections of the 1s2s ^{3}S level of He, the $2p^5 3s$ levels of Ne, and the $3p^5 4s$ levels of Ar using the Binary–Encounter–Bethe (BEB) model of Kim and Rudd [31].

Advanced theoretical methods such as *R*-matrix with pseudo-states, time-dependent close-coupling and perturbative distorted wave have been applied to helium, neon and argon [21–23] but are computationally difficult and thus have been limited to the low energies where ionization of only the valence electron needs to be considered. There is, therefore, a need for a simple model such as the BEB model that can be applied to complex atoms at all energies with much less computational effort. Further, the BEB model can provide ionization cross sections for levels with specific total angular momentum (J) values which can be used to study J-dependence of cross sections or combined to yield cross sections for an LS term (Russell–Saunders coupling) independent of J. As spin–orbit coupling becomes more important with increasing nuclear charge and strong coupling between the spin of the s valence electron and the core leads towards jK coupling, ionization cross sections from different levels arising from the same LS term are likely to be different.

The BEB model yields reliable cross sections for direct ionization of atoms and molecules and has been used with success

* Corresponding author. Tel.: +1 301 975 3211.
E-mail addresses: ali@nist.gov (M.A. Ali), pstone@nist.gov (P.M. Stone).

1387-3806/$ – see front matter. Published by Elsevier B.V.
doi:10.1016/j.ijms.2007.10.006

for a large number of systems [5] and thus is specially suitable for the present study. The method uses a simple formula and contains no adjustable parameters. The direct ionization cross section from the BEB model can also be augmented to include indirect ionization through excitation–autoionization for heavy atoms via the use of scaled Plane Wave Born excitation cross sections of autoionizing levels [7,32–34].

2. Theory and calculations

Kim and Rudd [31] developed the BEB model by combining the leading dipole part of the Bethe cross section [35] for high incident energy T with a modified form of the Mott cross section [36] for low T to obtain an expression for the singly differential ionization cross section with respect to ejected electron energy. They used a simple analytic form for the dipole continuum oscillator strength for an orbital. The expression for the BEB cross section for removing an electron occupying an orbital k by an incident electron of kinetic energy T is based on Eq. (57) of Kim and Rudd [31] and given explicitly as Eq. (5) by Hwang, Kim and Rudd [37]

$$\sigma_{\mathrm{BEB},k} = \frac{S}{(t+u+1)}\left[\frac{\ln t}{2}\left(1-\frac{1}{t^2}\right)+1-\frac{1}{t}-\frac{\ln t}{t+1}\right], \quad (1)$$

where $S = 4\pi a_0^2 N(R/B)^2$, $t = T/B$ is the normalized incident impact energy, $u = U/B$ is the normalized orbital binding energy, $a_0 = 0.5293 \times 10^{-20}\ \mathrm{m}^2$ (Bohr radius), and $R = 13.61$ eV (Rydberg energy). N is the number of electrons in the orbital k, B is the orbital binding energy, and $U = \langle p^2/2m\rangle$ is the orbital kinetic energy. The energies U and B are in general obtained from an atomic or molecular electronic structure computer program. The value of B for the valence orbital is the experimental ionization energy. Energies may be expressed in any convenient unit as only the dimensionless ratios of energies, t and u, appear in the equation.

The total ionization cross section in the BEB model is given by:

$$\sigma_{\mathrm{ion}} = \sum_k \sigma_{\mathrm{BEB},k} \quad (2)$$

where the summation is over all the occupied orbitals of the atom. The $t+u+1$ denominator on the right-hand side of (1) reduces the calculated cross section at low energies. At high energies, t becomes dominant in the denominator and the cross section becomes independent of $u+1$. Also at high energies, the bracketed terms in (1) are dominated by the $(\ln t)/2$ term and the cross section asymptotically approaches the first Born approximation [31]. The total cross section in the BEB approximation is therefore accurate at high energies and at energies near the threshold for ionization and connects smoothly in the peak region, all without any adjustable parameters.

Table 1
Experimental ionization energies of He (1s2s) ^{3}S and np^5($n+1$)s energy levels of Ne and Ar in eV [39]

Atom	Level	Ion	Level	Ionization energy (eV)
He	1s2s ^{3}S	He$^+$	1s ^{2}S$_{1/2}$	4.7678
Ne	2p^{5}3s ^{3}P$_2$	Ne$^+$	2p^5 ^{2}P$_{3/2}$	4.9495
	^{3}P$_1$			4.8937
	^{3}P$_0$			4.8492
	^{1}P$_1$			4.7165
Ar	3p^{5}4s ^{3}P$_2$	Ar$^+$	3p^5 ^{2}P$_{3/2}$	4.2113
	^{3}P$_1$			4.1360
	^{3}P$_0$			4.0365
	^{1}P$_1$			3.9315

We have obtained U and B for each orbital for each J from the Multi-configuration Dirac-Fock (MCDF) code of Indelicato and Desclaux [38]. A modification has been introduced into Eq. (1) to reduce the magnitude of $u+1$ in the denominator of Eq. (1) for atomic orbitals with principal quantum number $n \geq 3$. In earlier applications of the BEB model, Hwang et al. [37] found that the cross sections for these orbitals are reduced too much by the $u+1$ term because the kinetic energies of valence orbitals with many radial nodes are very large, leading to very low cross sections at energies close to threshold. The denominator on the right side of Eq. (1) is therefore replaced by $t+(u+1)/m$ where $m = 1$ when $n = 1, 2$ and $m = n$ when $n \geq 3$. The formula for BEB cross section thus becomes

$$\sigma_{\mathrm{BEB},k} = \frac{S}{t+(u+1)/m}\left[\frac{\ln t}{2}\left(1-\frac{1}{t^2}\right)+1-\frac{1}{t}-\frac{\ln t}{t+1}\right], \quad (3)$$

This expression is used for all the BEB cross sections in this work with appropriate values of m. In the MCDF calculations, the orbitals were optimized for each J separately within the 2p^5 3s Ne configuration and the 3p^5 4s Ar configuration. This allows us to investigate J-specific ionization cross sections. For the ^{3}P$_{2,1,0}$ levels, we calculated the lowest eigenvalue in each case, while for the ^{1}P$_1$ level we optimized on the second $J = 1$ eigenvalue. The ^{3}P$_2$ and ^{3}P$_0$ levels are metastable. The relevant observed energy levels of Ne and Ar arising from np^5 ($n+1$)s configurations for $n = 2$ and 3, respectively and the He 1s2s configuration are shown in Table 1 along with their ionization energies [39]. The wave functions for the $J = 1$ levels in jj coupling have mixed

Table 2
Configuration mixing of ^{3}P$_1$ and ^{1}P$_1$ levels in Ne and Ar in jj coupling and LS coupling. Columns 2 and 3 are wave function amplitudes for jj configurations, and columns 4 and 5 are projections onto the equivalent LS terms. The value of n is 2 for Ne and 3 for Ar

	(np$_{1/2}$)^2 (np$_{3/2}$)^3($n+1$)s	(np$_{1/2}$)^1 (np$_{3/2}$)^4($n+1$)s	LS ^{3}P$_1$	LS ^{1}P$_1$
2p^{5}3s ^{3}P$_1$	0.76499	−0.64404	−0.96752	0.25279
^{1}P$_1$	0.59879	0.80091	0.30823	0.95131
3p^{5}4s ^{3}P$_1$	0.89089	−0.45422	−0.88522	0.46517
^{1}P$_1$	0.42748	0.90403	0.49133	0.87097

Table 3
B and *U* values in eV for valence orbitals and *N* and *m* for Ne $2p^5 3s$ levels

Level	Orbital	*B*	*U*	*N*	*m*
$^3P_2$	$2p_{1/2}$	36.2440	130.823	2	1
	$2p_{3/2}$	36.6008	130.797	3	1
	3s	4.9445 *	7.2620	1	3
$^3P_0$	$2p_{1/2}$	37.7084	132.286	1	1
	$2p_{3/2}$	36.1376	130.370	4	1
	3s	4.8492*	7.2651	1	3
$^3P_1$	$2p_{1/2}$	36.6453	131.163	1.585	1
	$2p_{3/2}$	36.3853	130.619	3.415	1
	3s	4.8937*	7.1159	1	3
$^1P_1$	$2p_{1/2}$	37.0822	131.672	1.358	1
	$2p_{3/2}$	36.4609	130.579	3.642	1
	3s	4.7165*	7.2620	1	3

Experimental ionization potentials are marked with*.

electron configurations. The mixing increases from Ne to Ar as reflected in the wave function amplitudes of the configurations shown in Table 2. This mixing will be more pronounced in Kr and Xe.

3. Results

We display the *B* and *U* for the relevant metastable and excited levels for Ne and Ar in Tables 3 and 4 for the valence orbitals. The experimental ionization energy is used for *B* of the outermost orbital. These quantities are needed to calculate the BEB single ionization cross sections.

3.1. He 1s2s ^3S

1s2s ^{3}S and ^{1}S levels are metastable because they have the same parity as the ground configuration. To apply the BEB model to these levels, we need wave functions and *B* and *U* for 1s and 2s orbitals. We readily obtained the 1s and 2s orbitals for the ^{3}S level from the MCDF code as it is the lowest triplet level. The 1s2s ^{1}S level, however, is not the lowest singlet level and this causes convergence problems with the MCDF code. The MCDF and most atomic codes impose orthogonality between the 1s and 2s orbitals in a one configuration approximation and fail to yield a converged solution for the ^{1}S level. We have not been able, therefore, to apply the BEB method to this case. It is paradoxical that although numerous accurate wave functions for 1s2s singlet level are available, a very simple wave function for the BEB calculation eludes us. In a non-relativistic one-electron configuration description, the radial part of the wavefunctions for the 1s and 2s orbitals need not be orthogonal as the spin functions provide the orthogonality, as has been pointed out by Sharma and Coulson [40]. Sharma [41] and Rebelo and Sharma [42] have discussed the non-orthogonality problem in general and the effect of imposing orthogonality of the orbitals on the total wave function. Froese-Fischer [43] also has pointed out the importance of term-dependence of the 2s orbital when optimized on the singlet and the triplet level in extended calculations. Since we know the 2s orbitals for the singlet and triplet levels are different, we conjecture that the BEB ionization cross section for the singlet level is likely to be much different from and larger than that of the triplet as the convergent close coupling (CCC) results show [21,44].

It is interesting that the time-dependent close coupling (TDCC) configuration–average calculation [21] predicts the same cross sections for the singlet and triplet levels. We also note that the semiclassical Deutsch-Märk (DM) formalism [27] shows that the singlet cross sections are smaller than the triplet cross sections, in contrast to expected magnitudes. We list BEB ionization cross sections in Table 5 for the 1s2s $^3S_1$ level. We also display the cross sections in Fig. 1 and compare with other advanced theory results: distorted wave [21], CCC [44], and normalized Born [45]. We also show the experimental measurements of Dixon et al. [18,19]. The BEB cross section curve follows the CCC results (and TDCC results, not shown) at low impact energies up to 10 eV but lies lower. At higher energies, BEB cross sections are larger than CCC values and

Table 4
B and *U* values in eV for valence orbitals and *N* and *m* for Ar $3p^5 4s$ levels

Level	Orbital	*B*	*U*	*N*	*m*
$^3P_2$	$3p_{1/2}$	22.7356	87.4876	2	3
	$3p_{3/2}$	22.8087	87.6014	3	3
	4s	4.2113 *	7.2572	1	4
$^3P_0$	$3p_{1/2}$	23.6239	88.9012	1	3
	$3p_{3/2}$	22.5449	86.6817	4	3
	4s	4.0365*	7.2685	1	4
$^3P_1$	$3p_{1/2}$	22.8887	88.3002	1.794	3
	$3p_{3/2}$	22.7707	87.6959	3.206	3
	4s	4.1360*	6.8174	1	4
$^1P_1$	$3p_{1/2}$	23.4427	89.0905	1.183	3
	$3p_{3/2}$	22.7206	87.6420	3.817	3
	4s	3.9309*	5.8443	1	4

Experimental ionization potentials are marked with*.

Table 5
Ionization cross sections from He 1s2s ^{3}S at incident electron impact energies *T*

T	^{3}S	*T*	^{3}S
4.7678	0	35	4.7914
5.003	0.2240	40	4.5874
5.557	0.7683	50	4.1989
6.074	1.2619	60	3.8632
6.403	1.5584	75	3.4410
7.056	2.0972	90	3.1072
7.619	2.5076	100	2.9183
8.6	3.1096	150	2.2489
9.5	3.5534	190	1.9097
11.59	4.2818	248	1.5753
13	4.5992	348	1.2203
17	5.0624	400	1.0955
21	5.1778	500	0.9188
25	5.1354	650	0.7440
27	5.0836	750	0.6621
30	4.9847	850	0.5973
33	4.8712	1000	0.5219

Cross sections are in units of 10^{-20} m^2 and *T* is in eV.

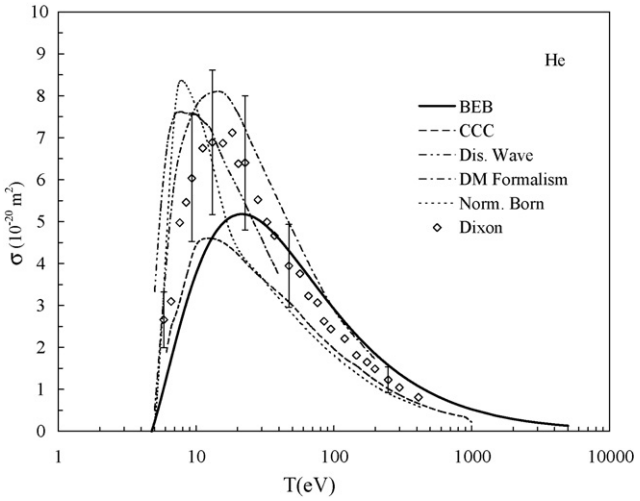

Fig. 1. Ionization cross sections for the He 1s2s ^{3}S level. Shown are the BEB values (solid line) of the present work; experimental measurements (diamonds) of Dixon et al. [18,19]; CCC results (dashed line) of Bray et al. [44]; the DM formalism (dot-dash line) of Deutsch et al. [27]; the distorted wave calculation (dot-dot-dash line) of Colgan an Pindzola [21]; and the normalized Born result (dotted line) of Beigman et al. [45]. Uncertainties of the measurements are shown at selected energies. All theories agree with the measurements at high energies.

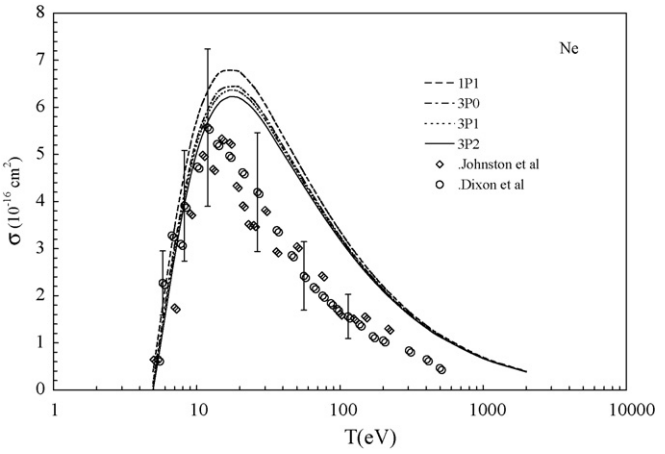

Fig. 2. Ionization cross sections of Ne $2p^5 3s$ levels. Shown are the BEB values of the present work for the $^3P_0$ and $^3P_2$ metastable levels and the $^3P_1$ and $^1P_1$ excited levels. All the levels have similar ionization cross sections as their electrons have similar binding energies. Circles are the experimental measurements of Dixon et al. [19] and diamonds are the measurements of Johnston et al. [20]. The BEB values approach the Born approximation asymptotically at energies above 1000 eV. Uncertainties of the Dixon et al. measurements are shown at selected energies.

Dixon et al. measurements and fall more slowly. The BEB cross section and Dixon et al. measurements peak at similar impact energy, but Dixon et al. values are much larger and close to distorted wave results. The normalized-Born results rise too steeply at low energy, are close to distorted wave results near the peak and follow the CCC results at high energy. The uncertainties of the experimental results of Dixon et al. (±25%) and divergence of the measurements from the theoretical results make it difficult to reach any conclusion about the validity of the theories. More experimental studies would help clarify the situation.

3.2. Ne $2p^5 3s$

We calculated BEB cross sections for ionization to the $2p^5$ $^2P_{3/2}$ Ne^+ ground level using the experimental ionization energies shown in Table 1 for *B* for the 3s orbital. The cross sections of metastable and excited levels are similar in magnitude and shape. The slightly different binding energies i.e., ionization energies, lead to slightly different peak values, the largest being from $^1P_1$ with the lowest ionization energy. These cross sections are shown in Fig. 2.

The Ne^+ $2p^5$ $^2P_{1/2}$ lies only 0.09676 eV higher than the $^2P_{3/2}$ level. The binding energy of the 3s orbital will therefore be higher by this amount for ionization to the $2p^5$ $^2P_{1/2}$ ion level. This increase of binding energy would lead to slightly lower cross sections and peak values for ionization to the $^2P_{1/2}$ level from these levels compared to ionization to the ion ground level. We show BEB cross sections for ionization to only the ground level of the ion in Fig. 2 and list these in Table 6.

If the experiment does not discriminate between the different levels of the ion produced, the $(2J+1)$ weighting and averaging of theoretical cross sections for both ion levels would also yield substantially the same cross sections. Thus, it is valid

Table 6
Ionization cross sections from Ne $2p^5 3s$ levels at incident electron impact energies *T*

T	$^3P_2$	$^3P_0$	$^3P_1$	$^1P_1$
4.945	0	0.1573	0.0795	0.3910
5	0.0809	0.2378	0.1638	0.4851
5.78	1.2487	1.4631	1.3686	1.7892
7	2.8163	3.0729	2.9653	3.4559
9	4.5066	4.7819	4.6702	5.1886
11	5.4315	5.7038	5.5944	6.1045
13	5.9152	6.1777	6.0722	6.5631
15	6.1453	6.3961	6.2948	6.7635
17	6.2265	6.4653	6.3683	6.8148
19	6.2185	6.4459	6.3529	6.7781
21	6.1568	6.3734	6.2843	6.6897
25	5.9498	6.1471	6.0650	6.4351
30	5.6327	5.8100	5.7353	6.0686
35	5.3110	5.4722	5.4036	5.7068
40	5.0306	5.1785	5.1147	5.3932
45	4.7858	4.9224	4.8630	5.1202
50	4.5654	4.6922	4.6367	4.8758
60	4.1859	4.2972	4.2479	4.4576
70	3.8120	3.9714	3.9271	4.1139
90	3.3841	3.4662	3.4291	3.5830
100	3.1903	3.2660	3.2317	3.3732
150	2.5133	2.5681	2.5428	2.6443
190	2.1699	2.2152	2.1942	2.2773
250	1.8173	1.8534	1.8365	1.9021
350	1.4479	1.4750	1.4622	1.5110
450	1.2133	1.2352	1.2247	1.2638
600	0.9840	1.0011	0.9920	1.0231
700	0.8769	0.8918	0.8847	0.9109
800	0.7923	0.8056	0.7993	0.8225
900	0.7237	0.7357	0.7300	0.7508
1000	0.6667	0.6777	0.6725	0.6914

Cross sections are in units of 10^{-20} m^2 and *T* is in eV.

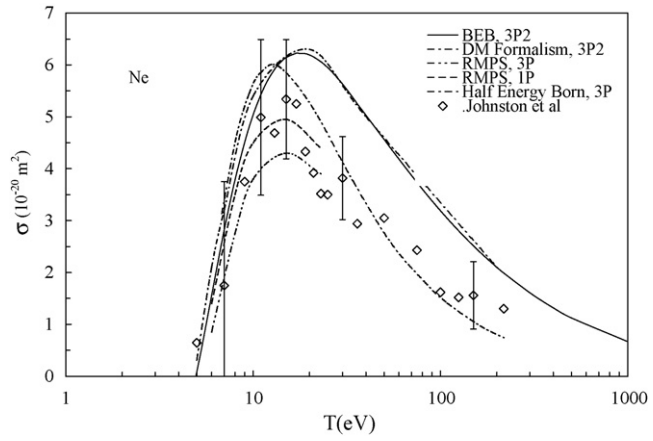

Fig. 3. Ne ionization cross sections compared with other theoretical values. The $^3P_2$ BEB results (solid line) are compared to the ^1P and ^3P *R*-matrix pseudo-state (RMPS) calculations (dashed and dot-dot-dash lines) of Ballance et al. [22]; the $^3P_2$ DM formalism (dot-dash line) of Deutsch et al. [27]; and the half energy Born calculations (dotted line) of Ton-That and Flannery [25]. Diamonds are the experimental measurements of Johnston et al. [20]. Uncertainties of the measurements are shown at selected energies.

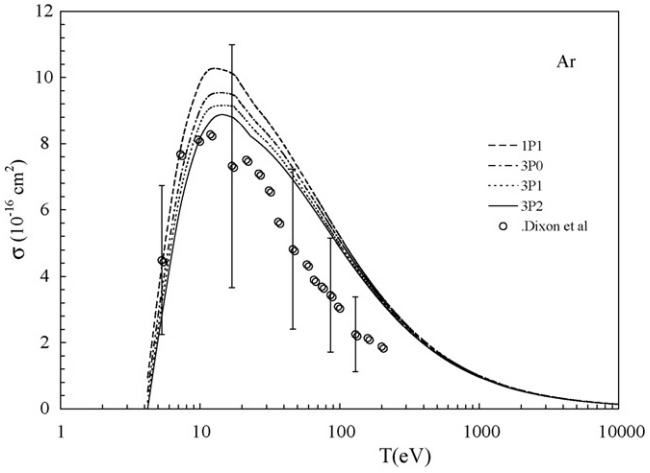

Fig. 4. Ionization cross sections of Ar $2p^5 3s$ levels. Shown are the BEB values of the present work for the $^3P_0$ and $^3P_2$ metastable levels and the $^3P_1$ and $^1P_1$ excited levels. All the levels have similar ionization cross sections as their electrons have similar binding energies. Circles are the experimental values of Dixon et al. [19]. The slight bulge in the BEB cross sections that begins at an energy of 23 eV is caused by the onset of ionization of the 3p inner shell of the atom. A similar bulge is evident in the experimental measurements. Uncertainties of the measurements are shown at selected energies.

to compare the cross sections in Fig. 2 with the experimental results of Johnston et al. [20] and Dixon et al. [19]. The BEB cross sections agree well with the measurements in the threshold region and up to about 15 eV. Above 15 eV, the calculated results are well above the measurement values. Measurement uncertainties are shown at selected energies for the Dixon et al. data.

We compare our BEB results with other theoretical calculations in Fig. 3. The BEB cross sections for the ^3P levels are about 20% higher than that of the *R*-matrix with pseudo-states (RMPS) results in the energy region of the peak cross section, and peaks at a slightly higher energy. TDCC results (not shown) are similar to the RMPS values [22]. A modified Born calculation (half energy Born) by Ton-That and Flannery [25] gives slightly larger values than the other calculations at low energies. Near the peak of the measured cross section and near the threshold energy, all the theoretical results are within the measurement uncertainties of Dixon et al. [19] and Johnston et al. [20]. At high energies, the BEB cross sections are about twice as high as the other calculations and the experiments. The BEB values asymptotically approach the Born cross section beyond about 1000 eV. Both the RMPS and TDCC are computationally difficult calculations and are limited to energies below 36 eV because they can only treat the valence 3s electron, neglecting ionization of the inner shell 2p electrons.

The semiempirical binary encounter method of Hyman [26] agrees with the measurements of Dixon et al. [19] at low energies but, like RMPS and TDCC, does not allow for ionization of the 2p electrons. The calculations are therefore limited to energies below about 36 eV. A Deutsch-Märk formalism [27] also gives reasonable agreement with the measurements, but includes weighting factors and low energy modifications to the formalism established for the rare gases.

3.3. Ar $3p^5 3s$

The BEB cross sections for ionization to $3p^5\ ^2P_{3/2}$ Ar^+ level are displayed in Fig. 4 and listed in Table 7. The BEB cross sections show more *J* dependence than in the case of Ne owing to the wider spread in their energy levels. The cross sections are also somewhat larger than the Ne cross sections, consistent with their smaller binding energies. As with Ne, the Ar BEB cross sections are in agreement with the experimental measurements of Dixon et al. [19] within the experimental uncertainties at the low energies and through the peak cross section region. At high energies, the BEB values are larger than the measurements by 20%–30%. It is valid, as in the Ne case, to use any of the four BEB curves for comparison with experimental values and other theoretical results.

Fig. 5 compares the BEB results for Ar with other theories. Only the $^3P_2$ result for BEB is shown, as it is representative of all the BEB results. The other theoretical results are for an average energy level or for a particular term rather then a specific level. All the theories are in agreement with experimental values at the lower energies and in the peak cross section region, within the measurement uncertainty. The RMPS results of Ballance et al. [22] are limited to energies below 21 eV because they do not include ionization from the 3p electron levels. The semiempirical binary encounter method of Hyman [26] agrees with the measurements of Dixon et al. [10] at low energies but does not allow for ionization of the 3p electrons above about 21 eV. A Deutsch-Märk formalism [27] also gives reasonable agreement with the measurements near the peak cross section but is high at larger energies and includes weighting factors and low energy modifications to the formalism that have been established for the rare gases. The half energy Born results of Ton-That and Flannery [25] agree with the measurements near the peak cross

Table 7
Ionization cross sections from Ar $3p^5 4s$ levels at incident electron impact energies T

T	$^3P_2$	$^3P_0$	$^3P_1$	$^1P_1$
4.211	0	0.5156	0.2097	0.9399
5.310	2.7894	3.5577	3.1484	4.2707
7.238	6.0936	6.9660	6.5280	7.8263
9.677	8.0121	8.8626	8.4416	9.7025
11.85	8.6748	9.4762	9.0779	10.2540
14	8.8745	9.6247	9.2489	10.3375
18	8.7261	9.3904	9.0521	9.9975
19	8.6394	9.2846	8.9547	9.8691
20	8.5428	9.1699	8.8481	9.7332
23	8.2315	8.8181	8.5081	9.3167
25	8.1146	8.6673	8.3750	9.1325
30	7.8231	8.3163	8.0502	8.7126
35	7.5316	7.9772	7.7328	8.3219
40	7.2468	7.6535	7.4276	7.9583
45	6.9740	7.3484	7.1382	7.6215
50	6.7159	7.0630	6.8664	7.3104
70	5.8353	6.1053	5.9487	6.2853
90	5.1588	5.3809	5.2504	5.5229
100	4.8785	5.0829	4.9622	5.2115
150	3.8548	4.0019	3.9138	4.0900
190	3.3156	3.4366	3.3637	3.5074
250	2.7544	2.8504	2.7922	2.9055
350	2.1655	2.2376	2.1937	2.2782
450	1.7950	1.8531	1.8177	1.8855
600	1.4380	1.4833	1.4556	1.5082
700	1.2735	1.3131	1.2888	1.3348
800	1.1447	1.1800	1.1584	1.1993
900	1.0410	1.0729	1.0534	1.0902
1000	0.9557	0.9847	0.9669	1.0004

Cross sections are in units of 10^{-20} m^2 and T is in eV.

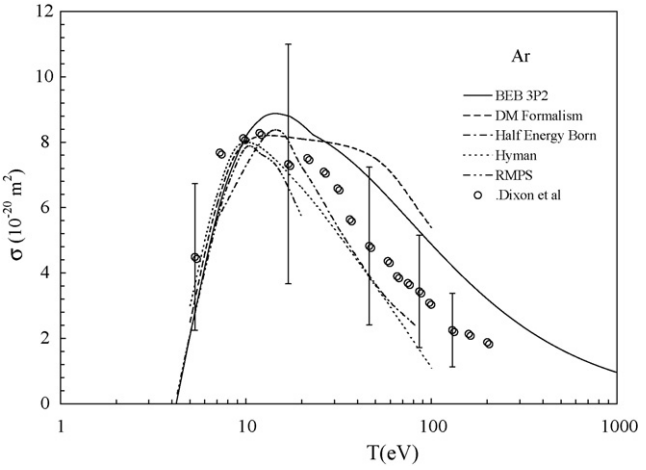

Fig. 5. Ar ionization cross sections compared with other theoretical values. The $^3P_2$ BEB results (solid line) are compared to the Deutsch-Märk (dashed line) formalism [27], the half energy Born (dot-dash line) values of Ton-That and Flannery [25], the semiempirical binary encounter theory (dotted line) of Hyman [26], and the RMPS results (dot-dot-dash line) of Ballance et al. [23]. Circles are the measurements of Dixon et al. [19]. Uncertainties of the measurements are shown at selected energies.

section but are low at higher energies. Their full Born calculation (not shown) is well above the measured peak cross section.

4. Conclusions

Electron impact ionization cross sections have been calculated for the first metastable states of He, Ne, and Ar by the BEB formalism. The results are in good agreement with experimental measurements and with more sophisticated and computer intensive theories from threshold through the peak cross section energies. At higher energies, the BEB cross sections are 20%–30% higher than measurements and more advanced theoretical results but will approach Born approximation values asymptotically. The BEB formalism, easily applied at all impact energies and without adjustable parameters, is particularly suitable for use in collisional–radiative models of gas discharges and plasmas.

Acknowledgement

This contribution is dedicated to the memory of Dr. Yong-Ki Kim in grateful thankfulness for years of collaboration and for sharing his insights, visions and enthusiasm for atomic physics and BEB method in particular. He was always thinking of fundamental extensions of BEB method while showing that the simple model is capable of yielding reliable data even for complex systems in a computationally frugal manner.

We appreciate helpful comments from Drs. J. Reader, C. Froese Fischer and P. Indelicato during the work. We acknowledge substantial help from Rodrigo Ibacache for digitizing diagrams from published papers for inclusion in our diagrams. This work was supported in part by the Office of Fusion Energy Sciences, U.S. Department of Energy. We would like to thank the Atomic Physics Group at the National Institute of Standards and Technology for its hospitality to allow us to work as guest scientists.

References

[1] L.J. Kieffer, G.H. Dunn, Rev. Mod. Phys. 38 (1966) 1, and references therein.
[2] T.D. Märk, G.H. Dunn, Electron Impact Ionization, Springer, Wien, 1985.
[3] R.S. Freund, in: L.C. Pitchford, B.V. McKoy, A. Chutijan, S. Trajmar (Eds.), Swarm Studies and Inelastic Electron Molecule Collisions, Springer, New York, 1987, p. 329.
[4] H. Deutsch, P. Scheier, K. Becker, T.D. Märk, Int. J. Mass Spectrom. 233 (2004) 13, and references therein.
[5] NIST website on ionization cross sections: http://physics.nist.gov/ionxsec and references therein.
[6] P. Bartlett, A.T. Stelbovics, At. Data. Nuc. Data Tables 86 (2004) 235.
[7] Y.-K. Kim, P.M. Stone, J. Phys. B: At. Mol. Opt. Phys. 40 (2007) 1597.
[8] R.S. Freund, R.C. Wetzel, R.J. Shul, T.R. Hayes, Phys. Rev. A 41 (1990) 3575.
[9] K.N. Joshipura, C.G. Limbachiya, Int. J. Mass. Spectrom. 216 (2002) 239.
[10] M.S. Pindzola, J. Colgan, F. Robicheaux, D.C. Griffin, Phys. Rev. A 62 (2000) 042705.
[11] E. Krishnakumar, S.K. Srivastava, J. Phys. B: At. Mol. Opt. Phys. 21 (1988) 1055.
[12] D. Rapp, P. Englander-Golden, J. Chem. Phys. 43 (1965) 1464.

[13] H.C. Straub, P. Renault, B.G. Lindsay, K.A. Smith, R.F. Stebbings, Phys. Rev. A 52 (1995) 1115.
[14] J. Vlacek, J. Phys. D: Appl. Phys. 22 (1989) 623.
[15] A. Boagaerts, R. Gijbels, J. Vlacek, J. Appl. Phys. 84 (1998) 121.
[16] A. Yanguas-Gil, J. Cotrino, A.R. Gonzalez-Elipe, Phys. Rev. E 72 (2005) 016401.
[17] A.J. Dixon, A. von Engel, M.F.A. Harrison, Proc. R. Soc. A 343 (1975) 333.
[18] A.J. Dixon, M.F.A. Harrison, A.C.H. Smith, J. Phys. B: At. Mol. Opt. Phys. 9 (1976) 2617.
[19] A.J. Dixon, M.F.A. Harrison, A.C.H. Smith, Contributed papers, eighth Int. Conf. on the physics of Electronic and Atomic Collisions (ICPEAC) Belgrade pp.405.
[20] M. Johnston, K. Fuffi, J. Nickel, S. Trajmar, J. Phys. B At. Mol. Opt. Phys. 29 (1996) 531.
[21] J. Colgan, M.S. Pindzola, Phys. Rev. A 66 (2002) 062707.
[22] C.P. Ballance, D.C. Griffin, J.A. Ludlow, M.S. Pindzola, J. Phys. B At. Mol. Opt. Phys. 37 (2004) 4779.
[23] C.P. Ballance, D.C. Griffin, M.S. Pindzola, S.D. Loch, J. Phys. B At. Mol. Opt. Phys. 40 (2007) F27.
[24] E.J. McGuire, Phys. Rev. A 26 (1982) 125.
[25] D. Ton-That, M.R. Flannery, Phys. Rev. A 15 (1977) 517.
[26] H.A. Hyman, Phys. Rev. A 20 (1979) 855.
[27] H. Deutsch, K. Becker, S. Matt, T.D. Märk, J. Phys. B At. Mol. Opt. Phys. 32 (1999) 4249.
[28] H. Deutsch, K. Becker, A.N. Grum-Grzhimailo, M. Probst, S. Matt-Leubner, T.D. Märk, Contri. Plasma Phys. 45 (2005) 494.
[29] D.A. Erwin, J.A. Kunc, J. Phys. B At. Mol. Opt. Phys. 36 (2003) 4605.
[30] D.A. Erwin, J.A. Kunc, Phys. Rev. A 70 (2004) 022705.
[31] Y.-K. Kim, M.E. Rudd, Phys. Rev. A 50 (1994) 3954.
[32] Y.-K. Kim, J.P. Desclaux, Phys. Rev. A 66 (2002) 012708.
[33] Y.-K. Kim, P.M. Stone, Phys. Rev. A 64 (2001) 052707.
[34] Y.-K. Kim, Phys. Rev. A 64 (2001) 032713.
[35] H. Bethe, Ann. Phys. 5 (1930) 325.
[36] N.F. Mott, Proc. Roy. Soc. A 126 (1930) 259.
[37] W. Hwang, Y.-K. Kim, M.E. Rudd, J. Chem. Phys. 104 (1996) 2956.
[38] P. Indelicato, J.P. Desclaux, Mcdfgme, a Multiconfiguration Dirac Fock and General Matrix Elements Program (release 2005), 2005, http://dirac.spectro.jissieeu.fr/mcdf.
[39] http://physics.nist.gov/PhysRefData/ASD/.
[40] C.S. Sharma, C.A. Coulson, Proc. Phys. Soc. 80 (1962) 81.
[41] C.S. Sharma, J. Phys. B 1 (1968) 1023.
[42] I. Rebelo, C.S. Sharma, J. Phys. B At. Mol. Phys. 5 (1972) 1286.
[43] C. Frose-Fischer, The Hartree-Fock Method for Atoms, John Wiley and sons, New York, 1977, p. 168.
[44] I. Bray, D.V. Fursa, A.S. Kheifets, A.T. Stelbovics, J. Phys. B At. Mol. Opt. Phys. 35 (2002) R117;
D.V. Fursa, I. Bray, J. Phys. B At. Mol. Opt. Phys. 36 (2003) 1663.
[45] I.L. Beigman, L.A. Vainshtein, M. Brix, A. Pospieszczyk, I. Bray, D.V. Fursa, Y.V. Ralchenko, At. Data Nucl. Data Tables 74 (2000) 123.